Abrupt equatorial wave-induced cooling of the Atlantic cold tongue in 2009

Gregory R. Foltz[1,2] and Michael J. McPhaden[3]

[1]   Between May and August 2009 sea surface temperatures (SSTs) in the eastern equatorial Atlantic dropped 5°C, from 1°C above normal to 1°C below normal. The magnitude of this cooling is unprecedented since satellite SST measurements began in 1982. In this study, observations and a linear equatorial wave model are used to examine the causes of the sharp decrease in SST. It is found that the anomalous cooling along the equator can be traced to an anomalous meridional gradient of SST and associated northwesterly anomalous winds that developed in the equatorial Atlantic the preceding spring. The anomalous winds forced upwelling equatorial Rossby waves that propagated westward during boreal spring and reflected at the western boundary into upwelling Kelvin waves during late spring and summer. The upwelling Kelvin waves propagated eastward along the equator, anomalously decreasing sea level and SST during May–August. **Citation:** Foltz, G. R., and M. J. McPhaden (2010), Abrupt equatorial wave-induced cooling of the Atlantic cold tongue in 2009, *Geophys. Res. Lett.*, *37*, L24605, doi:10.1029/2010GL045522.

1.   Introduction

[2]   The tropical Atlantic is influenced by two distinct modes of variability. The meridional mode is characterized by an anomalous meridional gradient of sea surface temperature (SST) centered near the latitude of the thermal equator (~5°N). Anomalous surface winds are directed toward the warmer hemisphere, resulting in a meridional displacement of the rain-producing intertropical convergence zone (ITCZ) [*Nobre and Shukla*, 1996]. The Atlantic Niño, on the other hand, consists of irregular warming of the eastern equatorial "cold tongue" of SST and is the Atlantic counterpart to the Pacific ENSO [*Zebiak*, 1993]. Ocean dynamics play a fundamental role in the Atlantic Niño, with positive coupled feedbacks between equatorial SST, zonal winds, and thermocline depth (i.e., Bjerknes feedback) tending to prolong and amplify individual Atlantic Niño events [*Carton and Huang*, 1994; *Keenlyside and Latif*, 2007].

[3]   There are important differences between the Atlantic Niño and Pacific ENSO that have implications for understanding equatorial Atlantic variability. Coupling between the ocean and atmosphere in the Atlantic is weaker than in the Pacific [*Keenlyside and Latif*, 2007]. As a result, external forcing from the equatorial Pacific and from the Atlantic subtropics likely plays a more important role in shaping the Atlantic Niño [*Chang et al.*, 2006; *Lübbecke et al.*, 2010; *Foltz and McPhaden*, 2010]. *Foltz and McPhaden* [2010] showed that surface wind anomalies associated with the Atlantic meridional mode generate equatorial Rossby waves during boreal spring. The Rossby waves reflect at the western boundary into equatorial Kelvin waves and propagate to the eastern equatorial Atlantic during boreal summer. These findings support previous results that emphasize the importance of wind-forced and western boundary generated equatorial waves in affecting the eastern equatorial Atlantic Ocean [*Illig et al.*, 2006; *Hormann and Brandt*, 2009].

[4]   During boreal spring 2009 anomalously warm SSTs and westerly surface wind anomalies developed in the equatorial Atlantic coincident with colder than normal SSTs in the tropical North Atlantic (Figure 1a). The resultant negative meridional interhemispheric SST gradient was the strongest of the past 30 years (Figure 1c). Between May and August, the period when the Atlantic Niño normally reaches its peak amplitude, equatorial Atlantic SSTs cooled 5°C, from 1°C above normal to 1°C below normal (Figure 1b). The magnitude of the anomalous cooling during May–August 2009 was unprecedented since satellite SST measurements began in 1982 (Figure 1d). The abrupt anomalous cooling was inconsistent with equatorial zonal winds, which were close to normal during June–August 2009 (Figures 1b and 2). In this study we examine the causes of the anomalous cooling, focusing on the role of oceanic equatorial waves.

2.   Data and Model

[5]   The combination of satellite data and a quasi-analytical linear equatorial wave model is used in this study. SST is available from the Tropical Rainfall Measuring Mission (TRMM) Microwave Imager (TMI) and the Advanced Microwave Scanning Radiometer for EOS (AMSR-E). These data are blended together using optimal interpolation and are available as daily averages on a 0.25° × 0.25° grid from June 2002 to the present from Remote Sensing Systems. We have regridded these data to a 1° × 1° resolution. We use the merged satellite sea level anomaly product from Archiving, Validation and Interpretation of Satellite Oceanographic data (AVISO). Sea level anomalies with respect to the 1993–1999 mean are generated on a 1° × 1° grid. Weekly averages are available from October 1992 through June 2006 and daily averages from July 2006 to the present. For consistency all data have been interpolated to a daily resolution. Previous studies have shown that interannual anomalies of

---

[1]Joint Institute for the Study of the Atmosphere and Ocean, University of Washington, Seattle, Washington, USA.
[2]Now at Atlantic Oceanographic and Meteorological Laboratory, NOAA, Miami, Florida, USA.
[3]Pacific Marine Environmental Laboratory, NOAA, Seattle, Washington, USA.

sea level in the eastern equatorial Atlantic are strongly positively correlated with thermocline depth anomalies [*Keenlyside and Latif*, 2007; *Hormann and Brandt*, 2009].

[6] Surface wind velocity from the SeaWinds instrument on the Quick Scatterometer (QuikSCAT) satellite is available from Institut Français de Recherche pour l'exploitation de la Mer (IFREMER)/Centre ERS d'Archivage et de Traitement (CERSAT) on a $0.5° \times 0.5° \times$ daily grid from July 1999 to November 2009. A blended satellite-in situ SST product [*Reynolds et al.*, 2002] is used to put the 2009 anomalies in perspective (Figure 1c). The rest of the analysis is restricted to the period Dec 2008–Oct 2009. Anomalies are calculated with respect to the daily mean climatology for the period 2003–2008, when all data sets are available.

[7] The linear wave model used in this study is described in detail by *Yu and McPhaden* [1999] and *Foltz and McPhaden* [2010]. Here we provide a brief summary. The
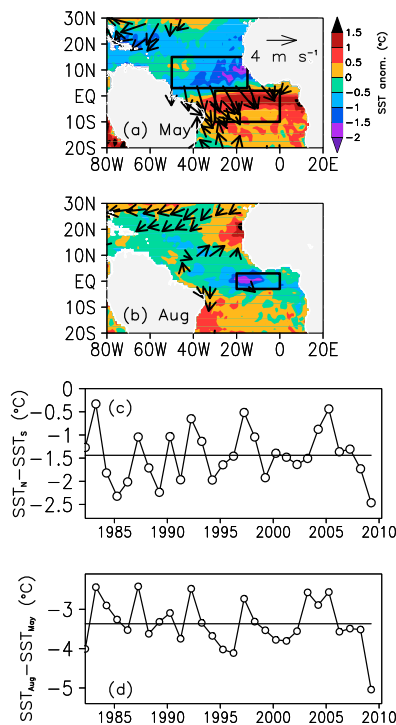

Figure 1. (a) Anomalies of SST (shaded) and surface winds (vectors, shown only where the wind speed anomaly is >1 m s^{-1}) during May 2009. Boxes indicate averaging regions used in Figure 1c. Here and in subsequent figures anomalies are calculated with respect to the 2003–2008 daily mean climatology. (b) Same as Figure 1a except for August 2009. Box indicates averaging region used in Figure 1d. (c) Difference of *Reynolds et al.*'s [2002] SST averaged in the tropical North Atlantic (2°N–15°N, 15°W–50°W) and South Atlantic (10°S–2°N, 0°–30°W) during April–May. (d) Difference between monthly *Reynolds et al.*'s [2002] SST in August and May of each year, averaged in the 0°–20°W, 3°S–3°N region shown in Figure 1b. Horizontal lines in Figures 1c and 1d are 1982–2009 mean SST differences. The cross-correlation between the time series in Figures 1c and 1d is 0.6, which is significant at the 99.9% level based on a 1000-sample permutation test.
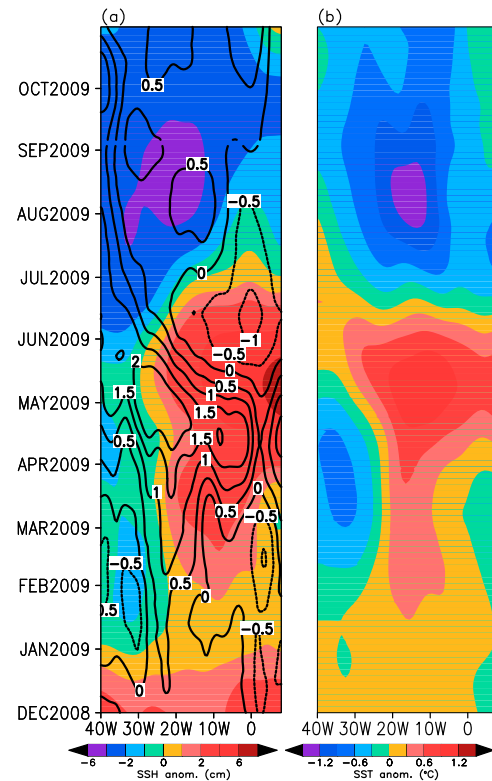

Figure 2. (a) Observed daily anomalies of sea level (shaded) and zonal wind stress (contours, 10^{-2} N m^{-2}) averaged in the 2°S–2°N band during Dec 2008–Oct 2009. (b) Same as Figure 2a except SST anomalies. All data here and in Figures 3 and 4 have been smoothed with a 20-day low-pass filter.

model is continuously stratified, and the longwave approximation has been made to filter out all waves except Kelvin and long Rossby waves. We have retained the first 10 baroclinic modes and 15 meridional modes (Kelvin plus first 14 Rossby). Phase speeds for the first and second baroclinic mode Kelvin waves are 2.3 and 1.4 m s^{-1}, respectively, and for the first and second baroclinic mode Rossby waves the phase speeds are 0.8 and 0.5 m s^{-1}, respectively.

[8] The model is unbounded in the meridional direction, and the zonal domain is 8°E–50°W, with meridional walls at the eastern and western boundaries. The reflection efficiency is set to 85% at the western boundary and 65% at the eastern boundary following *Foltz and McPhaden* [2010]. Despite the idealization of the eastern and western boundaries, the model reproduces observed variability of sea level in the equatorial Atlantic reasonably well during 2009 (Figure 3). The model also compares very well with a linear wind-driven numerical model that has more realistic coastal boundaries [*Foltz and McPhaden*, 2010] (Figure S1 of the auxiliary material).[1] The model is forced with daily QuikSCAT zonal wind stress during January 2000–October 2009. Output from 2001–2009 is used in this study to avoid transients associated with the first year of model spin up.

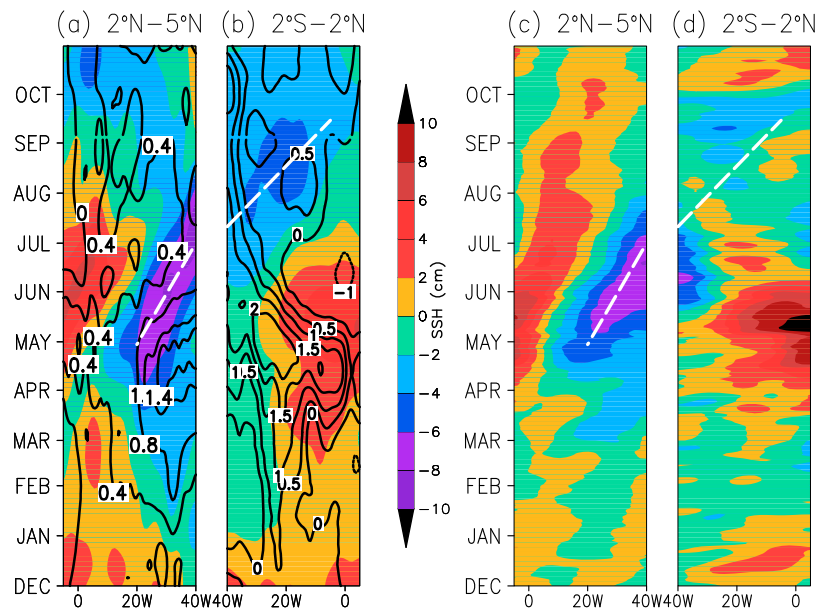[1]Auxiliary materials are available in the HTML. doi:10.1029/2010GL045522.

Figure 3. Observed sea level anomalies (shaded) during Dec 2008–Oct 2009 averaged between (a) 2°N–5°N and (b) 2°S–2°N. Contours in Figure 3a are Ekman pumping velocity in m day^{-1}, with positive values indicating upward velocity, calculated at a depth of 20 m by assuming a linear momentum balance as done by *Lagerloef et al.* [1999]. (b) Contours are zonal wind stress in 10^{-2} N m^{-2}. (c and d) Same as Figures 3a and 3b except sea level anomalies are from the linear wave model. The longitude axes in Figures 3a and 3c have been reversed to show reflection at the western boundary. Dashed white lines represent propagation speeds of observed negative sea level anomalies.

Wind stress is calculated using a constant drag coefficient of 1.8 × 10^{-3} and an air density of 1.29 kg m^{-3}.

3. Results

[9] In this section we investigate the causes of the anomalous cooling that occurred in the equatorial Atlantic during May–August 2009 (Figure 2). The cooling followed a period of anomalous warmth in the eastern equatorial Atlantic (0°–20°W) during January–May. The anomalous rise in SST was associated with westerly wind anomalies and above normal sea level in the equatorial band (Figure 2). The sea level and SST anomalies lagged the westerly wind anomalies by about one month, suggesting that the anomalous warming may have been driven by wind-induced deepening of the thermocline and associated reduction in turbulent cooling at the base of the mixed layer.

[10] During May–August 2009 SSTs cooled anomalously by ~2°C in the equatorial Atlantic (Figure 2b). The cooling occurred in conjunction with a transition from positive to negative sea level anomalies along the equator during June–July (Figure 2a). The strongest cooling was located in the central equatorial Atlantic near 15°W. There were westerly wind anomalies in the western basin at this time, which would favor generation of eastward-propagating downwelling Kelvin waves, tending to increase sea level and SST anomalously in the central and eastern equatorial Atlantic [*Servain et al.*, 1982]. It is therefore unlikely that the period of strongest anomalous cooling near 15°W was driven directly by equatorial winds, though there is a patch of anomalous easterly wind stress between 10°W–10°E during June–July that may have contributed to the anomalous cooling east of 10°W (Figures 2a and 2b).

[11] The cause of the anomalous cooling in the central basin during the boreal summer of 2009 instead can be traced to anomalous conditions that developed in the tropical North Atlantic during the previous spring. There was an anomalously negative meridional SST gradient during March–May (i.e., anomalously cold SSTs to the north of the equator relative to the south) and anomalous northwesterly surface winds along the equator (Figures 1a and 2a). The pattern of anomalous winds and SST is consistent with positive wind-evaporation-SST feedback [*Xie*, 1999]. The anomalous equatorial winds drove anomalous Ekman suction and negative sea level anomalies between 2°N–5°N (Figure 3a). The region of negative sea level anomalies propagated westward during April–June, presumably as a packet of equatorial Rossby waves. Sea level then decreased anomalously along the equator in the western basin during June–August (Figure 3b). There is evidence of eastward propagation of negative sea level anomalies on the equator between June and September, presumably as a result of equatorial Kelvin wave dynamics.

[12] To examine the role of equatorial waves in more detail, we consider the output from the linear wave model. The model captures the dominant features of the observed sea level variability during 2009 (Figures 3c and 3d). The westward-propagating negative sea level anomaly between 2°N–5°N is captured by the model. The observed and modeled amplitudes and phase speeds agree well, indicating that the westward propagation is due mainly to equatorial Rossby waves. The negative sea level anomalies on the equator are also captured by the model, though the amplitude is weaker in the model compared to observations (Figure 3d). The weaker amplitude in the model results partially from stronger than observed westward-propagating downwelling Rossby waves during June–August since these
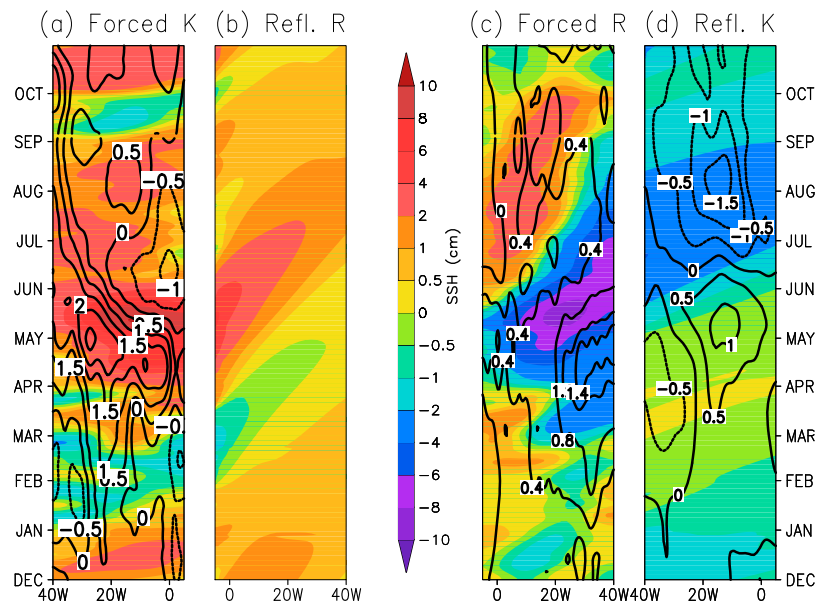
Figure 4. (a) Wind-forced Kelvin wave signal from the linear wave model (shaded) and observed zonal wind stress (contours, in 10^{-2} N m^{-2}) during Dec 2008–Oct 2009, averaged between 2°S–2°N. (b) Eastern boundary-reflected Rossby waves from the model, averaged 2°N–5°N. (c) Wind-forced Rossby waves from the model (shaded) and observed Ekman pumping velocity (contours, m day^{-1}) averaged between 2°N–5°N. (d) Western boundary-reflected Kelvin waves from the model (shaded) and observed SST anomalies (contours, °C), averaged between 2°S–2°N. Zonal scale has been reversed in (b) and (c) to show reflections at the eastern and western boundary, respectively.

waves have a modest sea level expression on the equator coherent with the stronger variability between 2°N–5°N. We have run a linear numerical model with realistic coastlines for the same time period and obtained similar results, suggesting that the discrepancy between observations and the quasi-analytical model output is not caused by the model's simplified coastline (Figure S1).

[13] The modeled off-equatorial sea level anomalies result from a superposition of the first and second baroclinic mode Rossby waves, each of which accounts for ~30–50% of the variability during 2009. The observed eastward phase speed of the negative sea level anomaly on the equator is ~0.8 m s^{-1}, which is significantly slower than the 1.4 m s^{-1} phase speed of second baroclinic mode Kelvin waves. The mismatch is likely due to the presence of westerly wind stress anomalies in the region of Kelvin wave propagation (Figure 3b). The strongest westerly wind anomalies centered near 15°W would force downwelling eastward-propagating Kelvin waves, giving the appearance of slower eastward propagation of the boundary-reflected negative sea level anomaly originating near the western boundary. Consistent with this interpretation, the eastward propagation of the negative sea level anomaly in the model is interrupted by a positive sea level anomaly between 0°–15°W during August that is driven by the westerly wind stress anomaly near 15°W (Figure 3d).

[14] One of the advantages of the quasi-analytical wave model is that its output can easily be separated into wind-forced and boundary-reflected components. The modeled positive sea level anomalies that developed on the equator during boreal spring of 2009 were associated mainly with wind-driven equatorial Kelvin waves (Figure 4a). The apparent lack of eastward propagation in the positive sea level signal is due to the combination of easterly wind stress anomalies in the eastern basin during June, which would tend

to lower sea level anomalously in the east, and westward propagation of the strongest westerly wind stress anomalies during April–June, tending to cause westward propagation of sea level. The downwelling Kelvin waves reflect into westward-propagating downwelling Rossby waves at the eastern boundary in April–June (Figure 4b).

[15] The same wind stress pattern that generates westerly anomalies on the equator produces anomalous Ekman suction between 2°N–5°N. The anomalous upwelling forces a packet of westward-propagating equatorial Rossby waves (Figure 4c) that reflect into upwelling equatorial Kelvin waves at the western boundary during May–August (Figure 4d). The reflected Kelvin waves propagate eastward along the equator, reaching the eastern boundary during June–September. The arrival of the upwelling Kelvin waves in the central and eastern equatorial Atlantic coincides well with the strongest observed anomalous cooling of SST, suggesting that the cooling was driven mainly by enhanced turbulent mixing associated with the wave-generated thermocline shoaling, which is in turn manifested in depressed sea levels (Figure 4d).

4. Summary and Discussion

[16] During boreal spring of 2009 SSTs were anomalously cold in the tropical North Atlantic and anomalously warm along the equator. SST anomalies warmer than 1°C occurred in the eastern equatorial Atlantic during the peak of this meridional SST gradient in May. Between May and August SSTs dropped 5°C along the equator, from 1°C above normal to 1°C below normal.

[17] This abrupt anomalous cooling during 2009 can be traced to the anomalous meridional SST gradient that was present during the preceding spring. Northwesterly wind

stress anomalies in the equatorial Atlantic associated with the SST gradient drove anomalous Ekman suction between 2°N–5°N. The resultant anomalous upwelling forced equatorial Rossby waves that propagated westward and reflected into eastward-propagating equatorial Kelvin waves at the western boundary. The reflected upwelling Kelvin waves reached the eastern equatorial Atlantic during boreal summer, causing the abrupt decrease in sea level and SST.

[18] Previous studies have found that interannual SST anomalies in the equatorial Atlantic are significantly affected by the dynamic response to direct zonal wind forcing mediated by equatorial Kelvin waves [*Illig et al.*, 2006; *Hormann and Brandt*, 2009; *Marin et al.*, 2009]. In contrast, the anomalous cooling in the summer of 2009 can be traced to the anomalous meridional SST gradient and northwesterly wind anomalies present during the preceding spring. Our results are consistent with those of *Foltz and McPhaden* [2010], who showed using data from 1993–2009 that equatorial Rossby waves generated by the meridional mode in boreal spring have a delayed negative feedback on the Niño mode in boreal summer. The extraordinary strength of the delayed negative feedback in 2009 and the resultant abrupt drop in equatorial SST is likely connected to the corresponding strength of the meridional SST gradient the preceding spring. The mechanisms responsible for generating the meridional SST gradient in 2009 are currently under investigation.

References

Carton, J. A., and B. H. Huang (1994), Warm events in the tropical Atlantic, *J. Phys. Oceanogr.*, *24*, 888–903.

Chang, P., et al. (2006), The cause of the fragile relationship between the Pacific El Niño and the Atlantic Niño, *Nature*, *443*, 324–328.

Foltz, G. R., and M. J. McPhaden (2010), Interaction between the Atlantic meridional and Niño modes, *Geophys. Res. Lett.*, *37*, L18604, doi:10.1029/2010GL044001.

Hormann, V., and P. Brandt (2009), Upper equatorial Atlantic variability during 2002 and 2005 associated with equatorial Kelvin waves, *J. Geophys. Res.*, C03007, doi:10.1029/2008JC005101.

Illig, S., et al. (2006), The 1996 equatorial Atlantic warm even: Origin and mechanisms, *Geophys. Res. Lett.*, *33*, L09701, doi:10.1029/2005GL025632.

Keenlyside, N. S., and M. Latif (2007), Understanding equatorial Atlantic interannual variability, *J. Clim.*, *20*, 131–142.

Lagerloef, G. S. E., G. T. Mitchum, R. B. Lukas, and P. P. Niiler (1999), Tropical Pacific near-surface currents estimated from altimeter, wind, and drifter data, *J. Geophys. Res.*, *104*, 23,313–23,326.

Lübbecke, J. F., C. W. Böning, N. S. Keenlyside, and S.-P. Xie (2010), On the connection between Benguela and equatorial Atlantic Niños and the role of the South Atlantic Anticyclone, *J. Geophys. Res.*, *115*, C09015, doi:10.1029/2009JC005964.

Marin, F., et al. (2009), Why were sea surface temperatures so different in the eastern equatorial Atlantic in June 2005 and 2006?, *J. Phys. Oceanogr.*, *39*, 1416–1431.

Nobre, C., and J. Shukla (1996), Variation of sea surface temperature, wind stress, and rainfall over the tropical Atlantic and South America, *J. Clim.*, *9*, 2464–2479.

Reynolds, R. W., N. A. Rayner, T. M. Smith, D. C. Stokes, and W. Q. Wang (2002), An improved in situ and satellite SST analysis for climate, *J. Clim.*, *15*, 1609–1625.

Servain, J., J. Picaut, and J. Merle (1982), Evidence of remote forcing in the equatorial Atlantic Ocean, *J. Phys. Oceanogr*, *12*, 457–463.

Xie, S.-P. (1999), A dynamic ocean-atmosphere model of the tropical Atlantic decadal variability, *J. Clim.*, *12*, 64–70.

Yu, X., and M. J. McPhaden (1999), Seasonal variability in the equatorial Pacific, *J. Phys. Oceanogr.*, *29*, 925–947.

Zebiak, S. E. (1993), Air-sea interaction in the equatorial Atlantic region, *J. Clim.*, *6*, 1567–1586.

G. R. Foltz, Atlantic Oceanographic and Meteorological Laboratory, NOAA, 4301 Rickenbacker Cswy., Miami, FL 33149, USA. (gregory.foltz@noaa.gov)

M. J. McPhaden, Pacific Marine Environmental Laboratory, NOAA, 7600 Sand Point Way NE, Seattle, WA 98115, USA.